CHAPTER IV

RESULTS

Part I: The basic characteristic of the cell lines:

4.1. Cell morphology

4.1.1 AMC-K46

According to 3.3.1.1, AMC-K46 (18th passage) exhibited 3 different cell types; epitheloids, fibroblastoids and giant cells (Figure 4.1). The epitheloid cells, polygonal shape, predominantly presented (86% of cell population) in the cultures with 25-50 μm in diameter. The fibroblastoid cells were 35-65 μm in length with slender or finger-like shape with 11 % of appearance. The giant cells, large polygonal shape, were fewly found, 75-110 μm in diameter. The 3 cell types were well stained with Giemsa and presented with 1-3 nucleolus (Figure 4.2). The epitheloids and the fibroblastoids were mononucleated and the giant cells contained two or more nuclei. The cytoplasm of the cells was stained in blue with purple nucleus and light blue nucleolus.

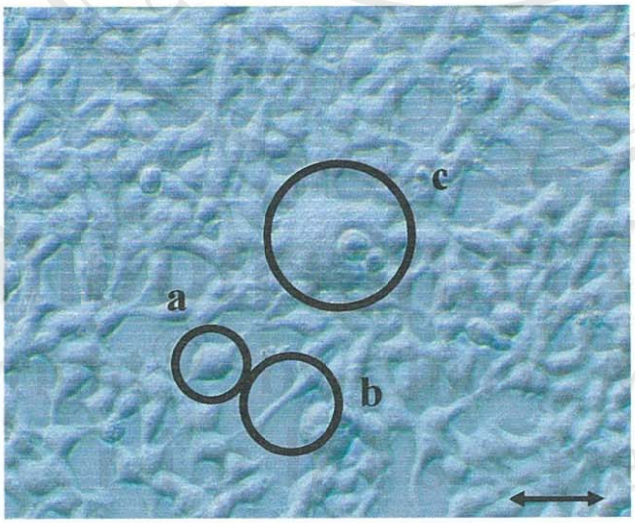

Figure 4.1 AMC-K46 morphology; (a) epitheloid, (b) fibroblastoid and (c) giant cell (phase-contrast inverted microscope) (scale bar = 50 μm)

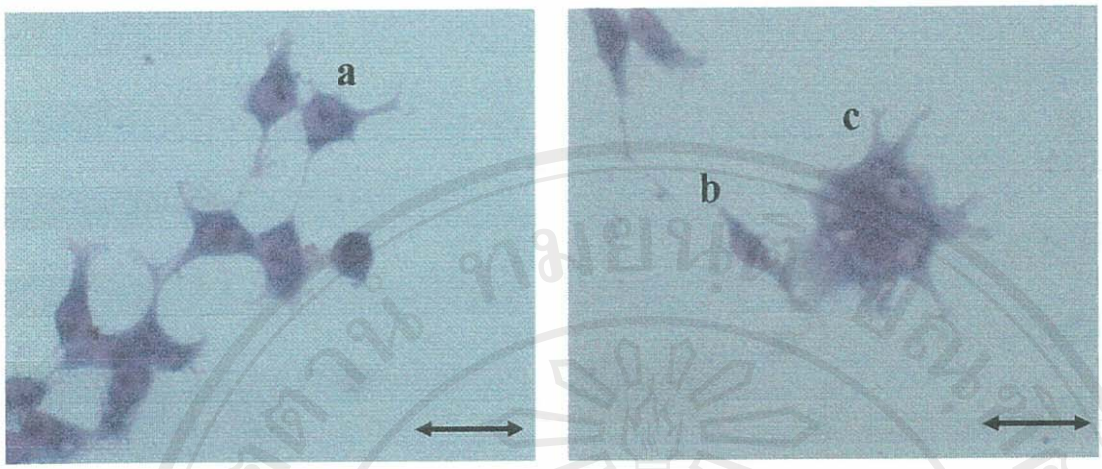

Figure 4.2 AMC-K46 stained with Giemsa; (a) epitheloid, (b) fibroblastoid and (c) giant cells (scale bar = 50 µm)

4.1.2 HeLa

The unicharacter morphology of HeLa contains the epitheloid cells with 45-60 µm in diameter (Figure 4.3). HeLa grows in 1-2 layers with highly proliferative activity. The Giemsa stained cells contain a light purple nucleus with 3-6 blue nucleoli and the purple cytoplasm with clearly define edge.

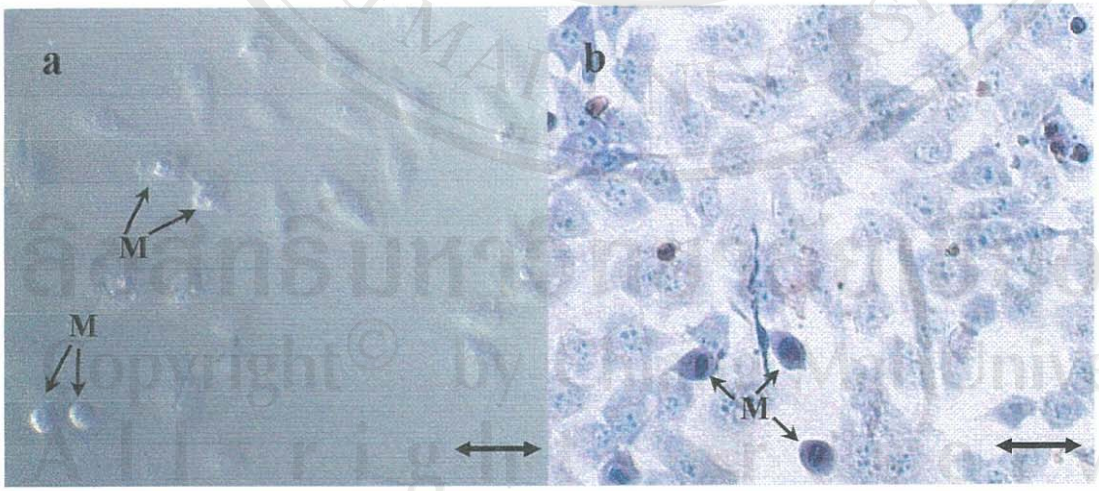

Figure 4.3 HeLa morphology; (a) living cells and (b) Giemsa stained cells. The mitotic cells (M) could be distinguished from the surrounded resting cells. (scale bar = 50 µm).

4.2 The growth pattern of the two cell lines

4.2.1 The growth pattern of AMC-K46 was studied within 8 days and presented in Figure 4.4. The 2 phases of the growth pattern were shown; log phase (exponential phase) and stationary phase (plateau phase). After the day of seeding (the innoculum size, $2x10^4$ cell/cm^2), AMC-K46 exhibited 5 days in log phase. The doubling time was approximately 40-48 hours on the midlog phase. The Plateau phase was observed after the 5th day with the confluent density approximately $1.13x10^5$cells/cm^2 (Figure 4.5).

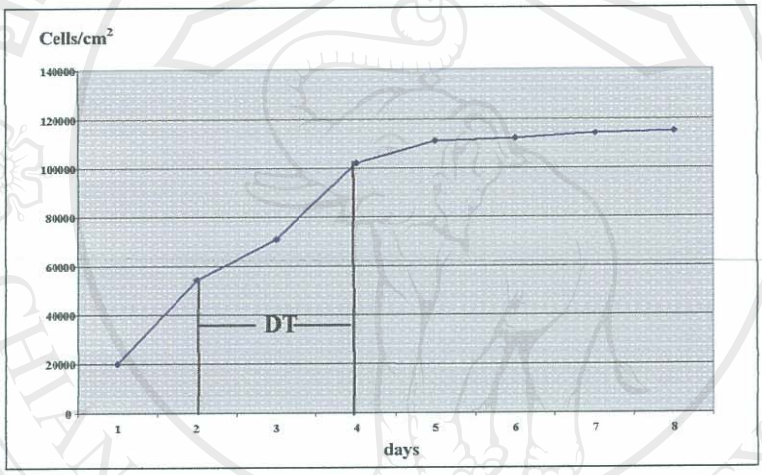

Figure 4.4 Growth pattern of AMC-K46. The lag phase was not exhibited by the cells in this study. The doubling time (DT) was approximately 2 days (or 48 hours).

Figure 4.5 The confluent stage of AMC-K46 with 1.13×10^5 cells/cm^2 was observed under the inverted microscope. (scale bar = 100 µm)

4.2.2 HeLa growth pattern shown in Figure 4.6. The cells were seeded with $2x10^4$ cells/cm^2 and the typical growth pattern was presented with the 3 phases; lag phase, log phase and Plateau phase. The lag phase was 24-48 hours and the Plateau phase exhibited after the 8th day. The doubling time was approximately 24 hours. The confluent stage of the cells was approximately $1.86x10^5$ cells/cm^2 (Figure 4.7).

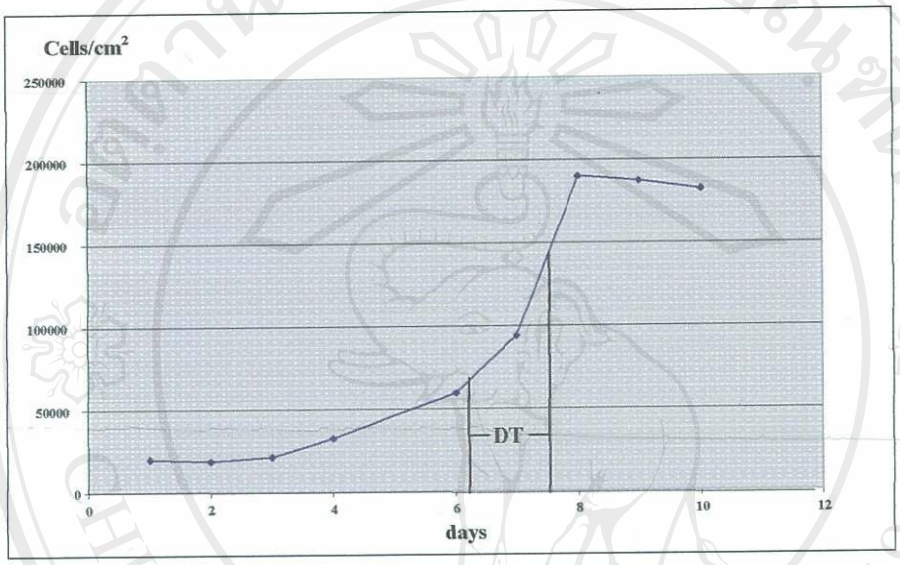

Figure 4.6 The growth pattern of HeLa (DT = doubling times).

Figure 4.7 The confluent stage of the HeLa with 1.86×10^5 cells/cm^2. (scale bar = 100μm)

4.3 Karyotype and G-banding of AMC-K46

The karyotype of AMC-K46 was screened from 100 spreading metaphases in passage 18th according to ISCN (see introduction). The cells expressed aneuploidy with the chromosome number ranged between 46 to 136 and the frequency of chromosome number pattern has shown in Figure 4.8. The metaphase of 46 and 136 chromosome has shown in Figure 4.9. The cells with 67 and 68 chromosome were found with the highest frequency at 18% and 17% respectively. The metaphases with 67 was chosen as the modal chromosome number in this study. The distribution of chromosome number in the 67 and 68 was summarized in Table 4.1. Many types of chromosome markers have been identified from M1- M13 with only a few in common among the cells with different number of chromosome. The results of G-bandings study indicated the identification of the chromosome number and categorized the chromosome by ordinal number or karyotype (see Figure 4.10 – 4.19). The karyotype of the AMC-K46 expressed the true mosaicism. There were chromosome aberrations appeared in the cells including; numerical changes (the randomly increasing or decreasing of the number of chromosome on the ordinal chromosome number) and structural changes (13q+ in M1 or translocaton in M11). The conclusion could be proposed in this study that both of the chromosome aberrations could be used to evaluate the effect to the plant extracts to AMC-K46 (see 4.5.3).

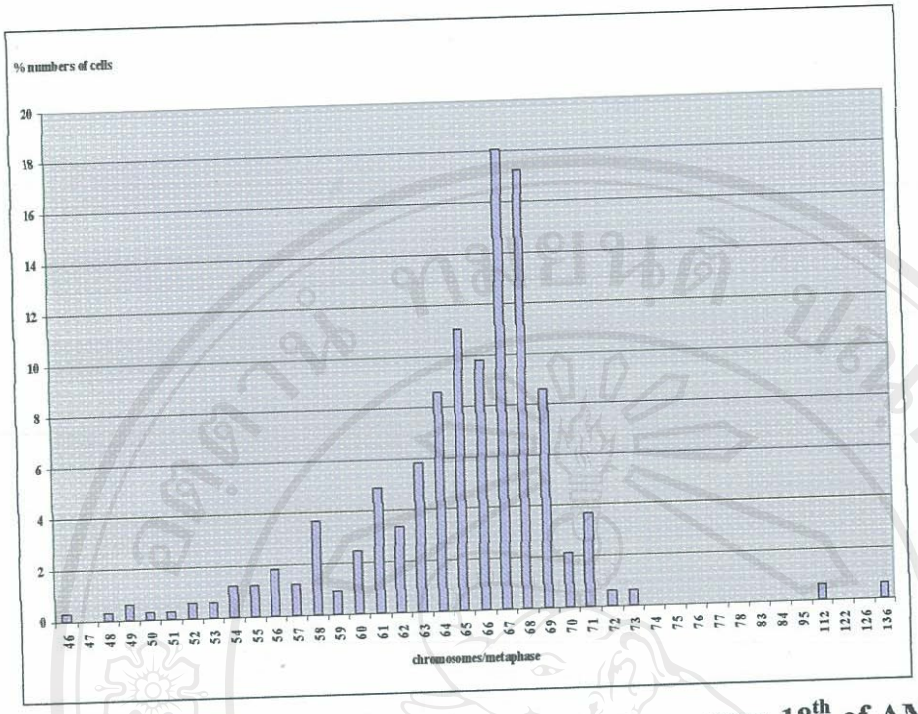

Figure 4.8 The total chromosome number pattern on passage 18th of AMC-K46 ranging from 46 to 136. The highest frequency chromosome number was 67 (18%).

a) **b)**

Figure 4.9 The metaphase of AMC-K46 with a) 46 and b) 136 chromosome (Giemsa stained).

Number of chromosome per metaphase		Chromosome ordinal number increased	Chromosome ordinal number decreased	Type of chromosome marker	Related figure of karyotype
67	(a)	4, 6, 7, 8, 10, 16, 17, 19, 20 , 21 and X	Y	M1 M2 M3 M4	4.10
	(b)	1, 2, 3, 5, 6, 8, 11, 12, 14, 16, 17, 19, X and Y	-	M5 M6	4.12
68	(a)	1, 2, 3, 4, 5, 6, 7, 8, 11, 12, 15, 18, 19, 20 and 21	9, 14, 22 and Y	M1 M7 M8	4.14
	(b)	1, 2, 3, 5, 6, 7, 8, 10, 11, 12, 14, 18, 19, 20 21, X and Y	9, 13 and 22	M1 M9 M10	4.16
	(c)	3, 4,5, 6, 7, 10, 15, 16, 19, 21 and 22	14, 18 and 20	M1 M11 M12 M13	4.18

Table 4.1 The summarization of the highest frequency of the chromosome (67 and 68) of AMC-K46, which 67 was chosen as the modal chromosome number.

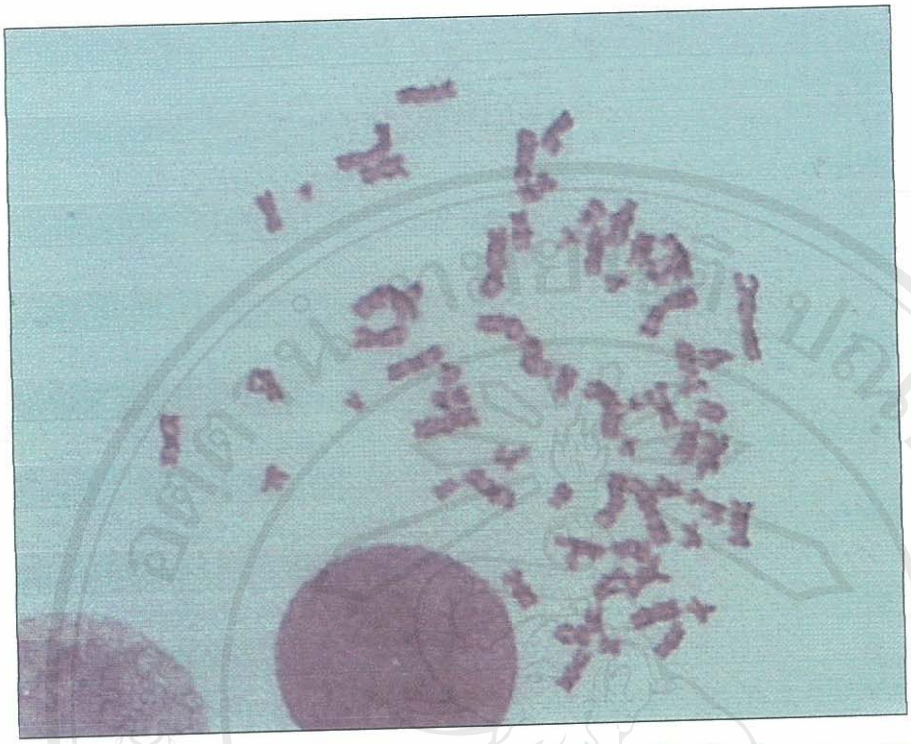

Figure 4.10 The G-banding metaphase of AMC-K46 with 67 chromosomes (67 (a)).

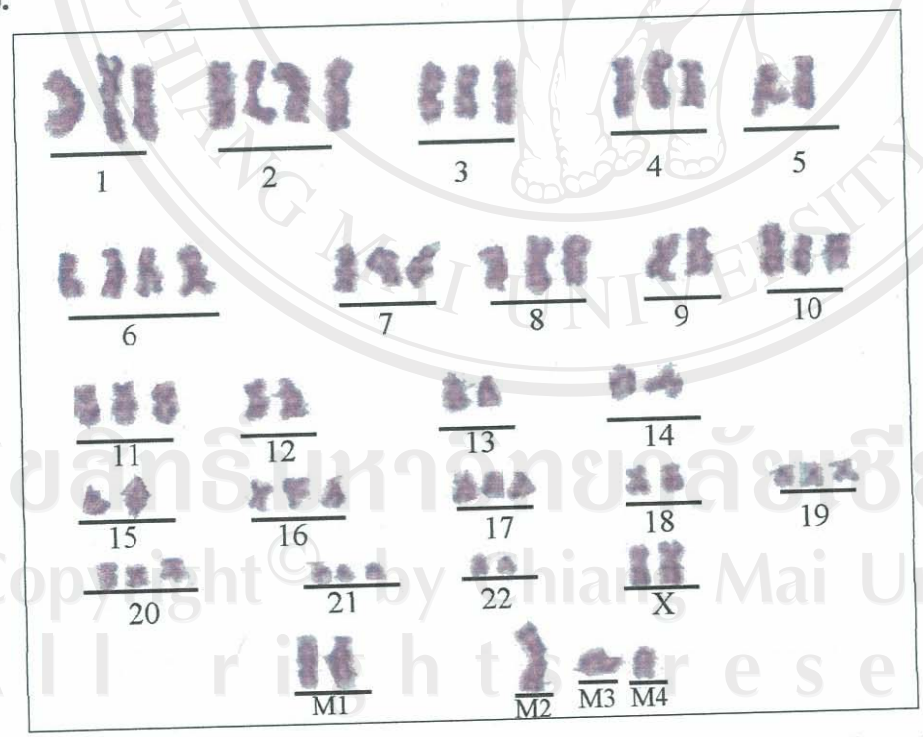

Figure 4.11 The karyotype of Figure 4.10: notice the increasing number of the chromosome 4, 6, 7, 8, 10, 16, 17, 19, 20, 21 and X with the 4 marker chromosomes (M1, M2, M3 and M4) and the Y was disappeared.

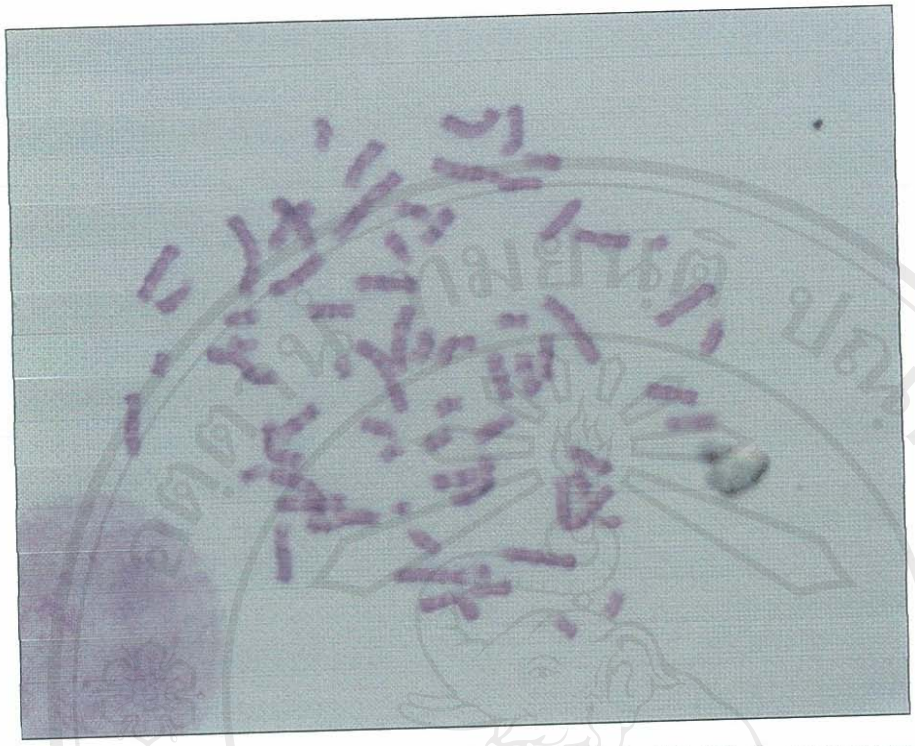

Figure 4.12 The G-banding metaphase of AMC-K46 with 67 chromosomes (67 (b)).

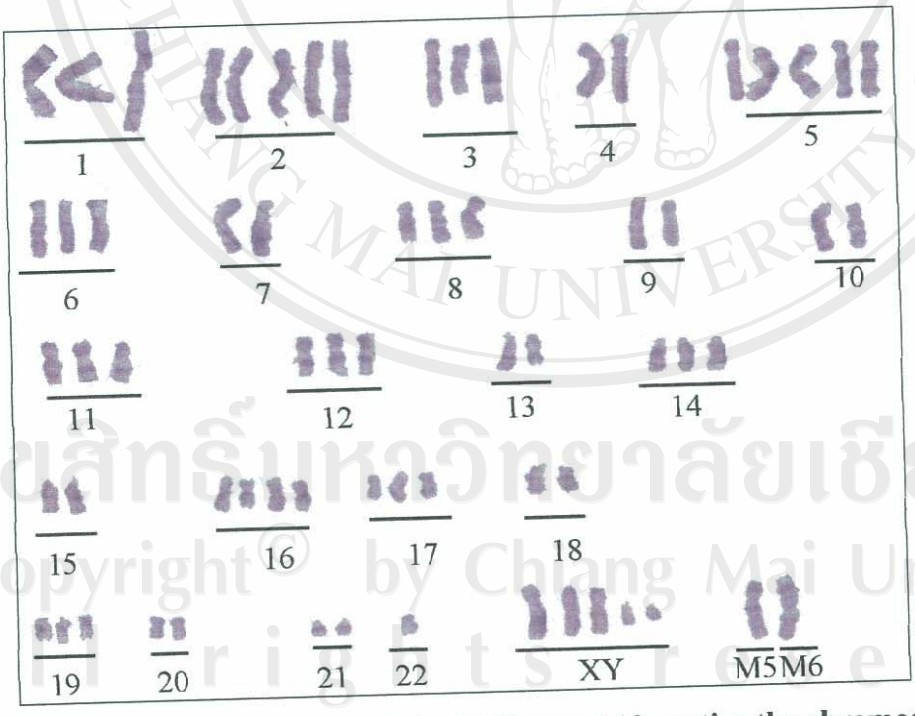

Figure 4.13 The karytype of metaphase in Figure 4.12: notice the chromosomes 1, 2, 3, 5, 6, 8, 11, 12, 14, 16, 17, 19, X and Y were increased, while the non-specific chromosomes were decreased and 2 marker chromosomes were found (M5 and M6).

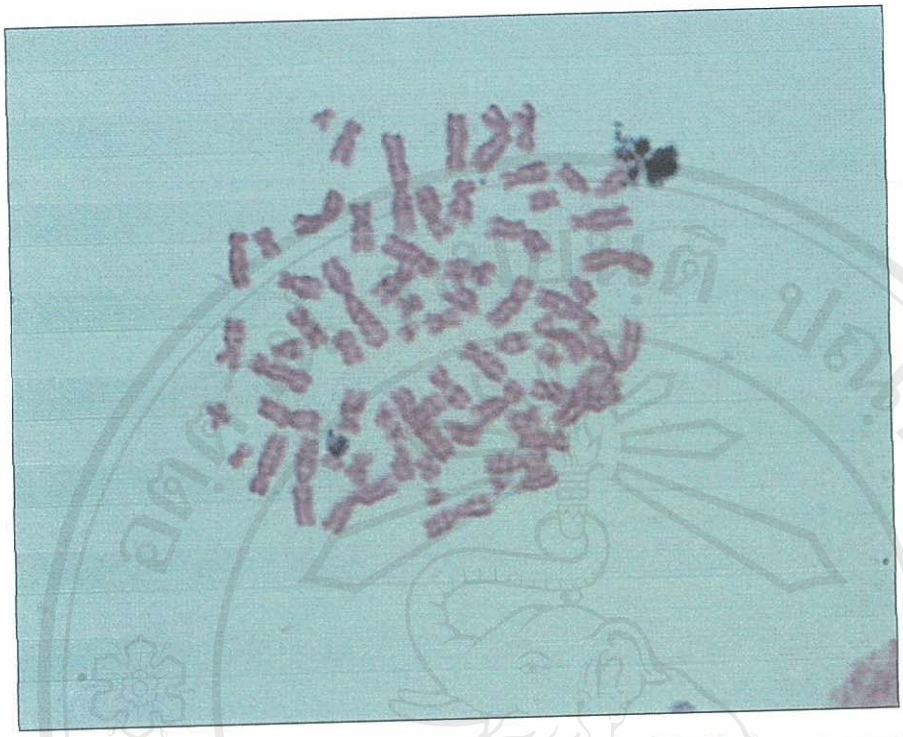

Figure 4.14 The G-banding metaphase of AMC-K46 with 68 chromosomes (68 (a)).

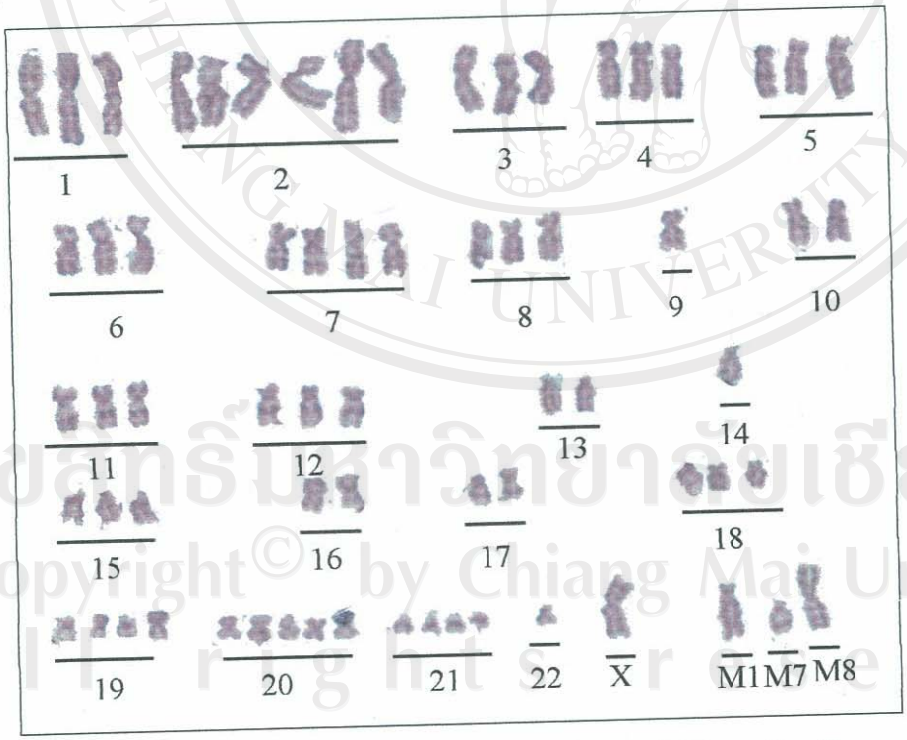

Figure 4.15 The karyotype of the metaphase in Figure 4.14: notice the chromosomes 1, 2, 3, 4, 5, 6, 7, 8, 11, 12, 15, 18, 19, 20 and 21 were increased, while the chromosomes 9, 14 and 22 were decreased, the Y was disappeared and the makers M1, M7 and M8 were found.

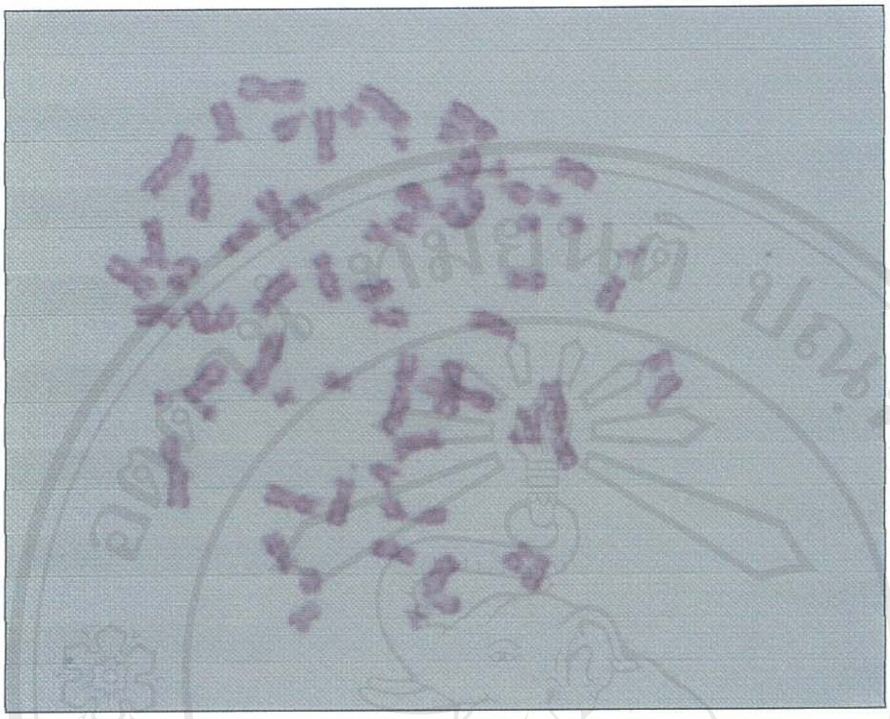

Figure 4.16 The G-banding metaphase of AMC-K46 with 68 chromosomes (68 (b)).

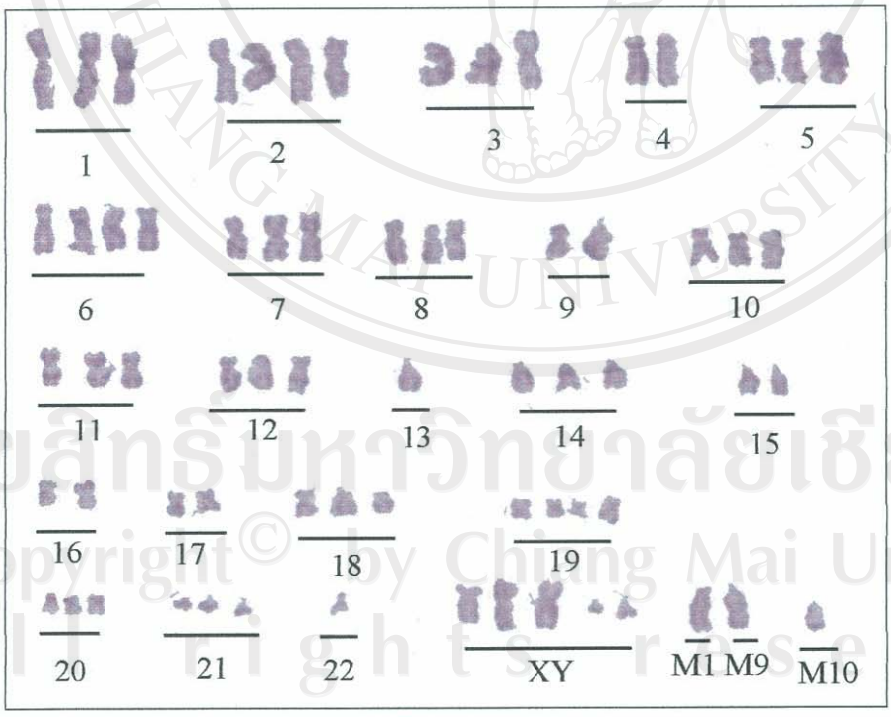

Figure 4.17 The karyotype of the metaphase in Figure 4.16: notice the chromosomes 1, 2, 3, 5, 6, 7, 8, 10, 11, 12, 14, 18, 19, 20 21, X and Y were increased, while the chromosomes 13 and 22 were decreased and M1, M9 and M10 were found.

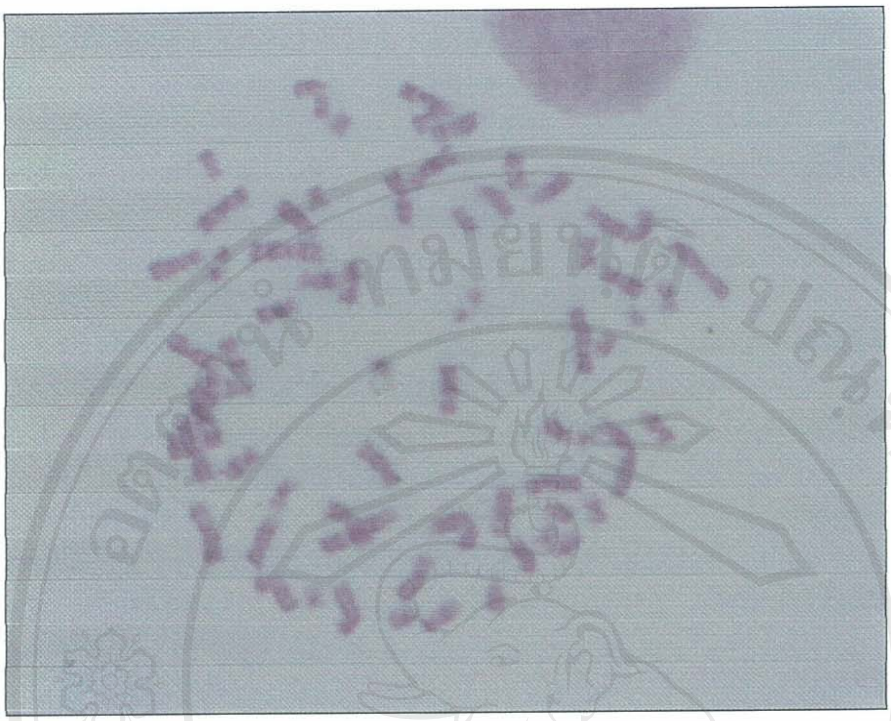

Figure 4.18 The G-banding metaphase of AMC-K46 with 68 chromosomes (68 (c)).

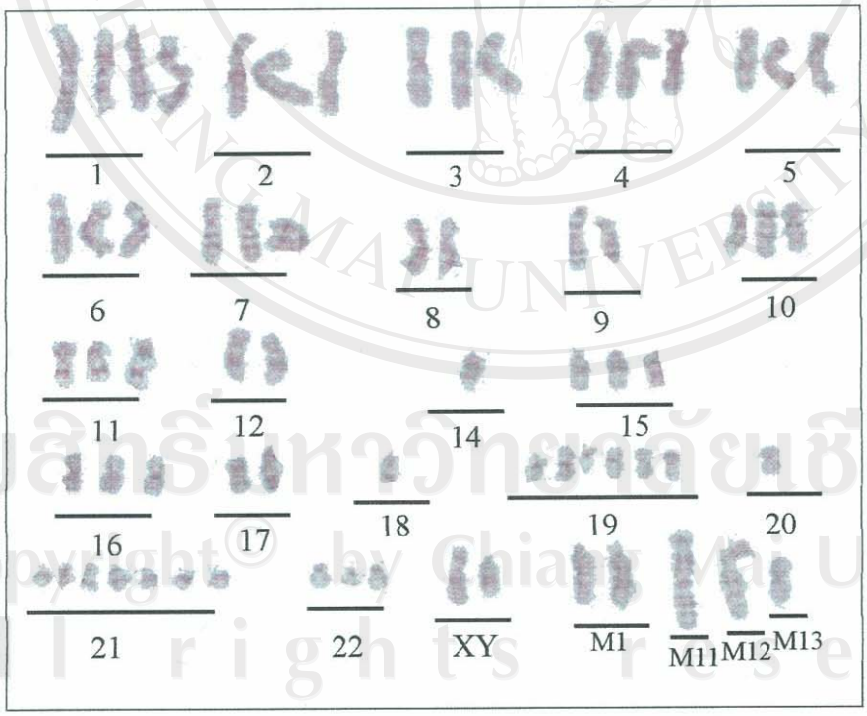

Figure 4.19 The karyotype of AMC-K46 from Figure 4.18: notice the increasing number of chromosomes 3, 4, 5, 6, 7, 10, 15, 16, 19, 21 and 22, while the decreasing number of chromosomes 14, 18 and 20 and the 4 markers were found (M1, M11, M12 and M13).

Part II : The cytotoxicity of the plants crude extract to the cell lines

4.4 MTT assay condition studied

4.4.1 Dividing and non-dividing condition

The relationship between the MTT optical density (OD_{MTT} 570/620) and the cell density of the two cell lines has been evaluated according to 3.3.2.3 (1). The two cell lines exhibited a similar pattern of relationship (Figure 4.20). Pattern of relationships are the representative and outlining of their growth profile; they were used in this research to ensure the correct phases of growth, the exponential or the stable. On the exponential phase, the optical densities (ODs) were exponentially increased depending on the cell densities up to 9×10^4 and 7×10^4 cells/well for AMC-K46 and HeLa respectively. The narrow fluctuation of ODs (or, in the other words, the stable ODs) were observed in both cell lines on the higher cell densities, stable phase, ranging between 0.8×10^5-1.5×10^5 and 0.5×10^5-0.9×10^5 for AMC-K46 and HeLa respectively. The first value of cell densities at the beginning of stable ODs was indicated in this research as the "confluent density" (Figure 4.20); *i.e.* on 9×10^4 and 7×10^4 cells/well for AMC-K46 and HeLa respectively. This pattern of relationship should be explained by the characteristics (monolayer and contact inhibition) of both cell lines which were discussed below.

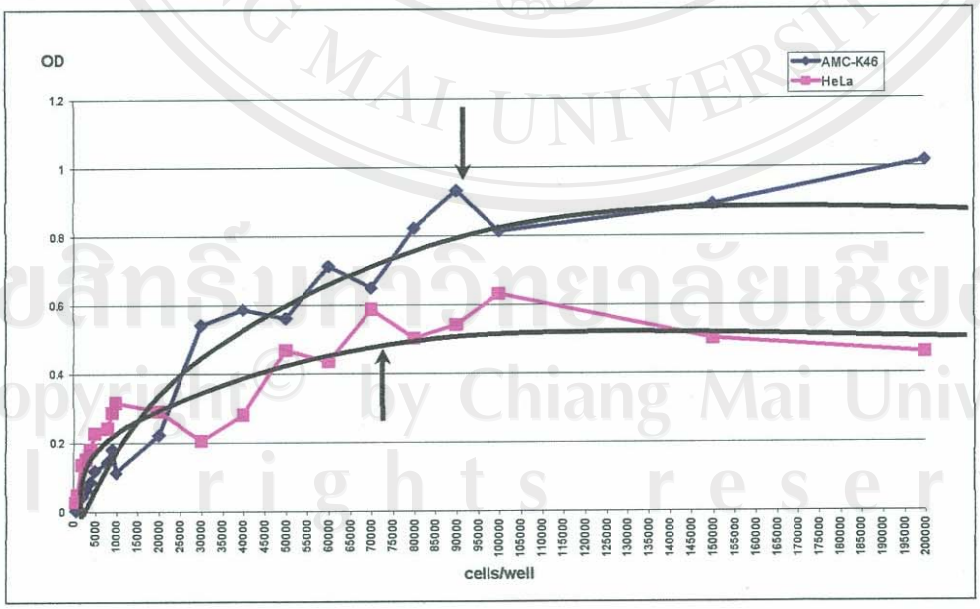

Figure 4.20 The relationship between the MTT optical density (OD_{MTT} 570/620 nm) and the density of the cells. The arrows indicated the position of the confluent densities (see text) of both cell lines (AMC-K46 and HeLa).

There was no previous report available to explain clearly about the relationship between the MTT optical densities (OD_{MTT}) and the characteristics (monolayer and contact inhibition) of the animal cells. A hypothesis is proposed in this study to explain the biology of such a relationship. The exponential phase of the curve (Figure 4.20) represented the increasing of the cell density and with the gradually depletion of space among the attached cells. The confluent condition (no cell division) occurred at cell density approximately greater or equal to 9×10^4 and 7×10^4 cells/well (*i.e.* the confluent density) for AMC-K46 and HeLa respectively. The exceeded population of the cells on the stable ODs could not attach to the monolayer, but dwelled as cell suspension and washed away during the treatments and the MTT assay. The stable OD_{MTT} was therefore become the indicatives of the confluent density of the cells in the wells of cultured plate. The above evidences needed more study to support using the other cell lines with monolayer type and with contact inhibition character, such as 3T3. However, such a study was beyond the scope of this research and has not been done so far.

The optimum densities of the dividing and non-dividing density (Table 4.2) of both cell lines were determined from two microscopic configurations of the cells; (i) the space among the attached cells after seeding and (ii) the size of the cells. According to the size of both cells the optimum spaces among the cells was determined at approximately 100 - 150 μm which allowed the possibility of 2-3 generations of cell division. The size of HeLa is generally larger than that of the AMC-K46 (see 4.1) and therefore the dividing density of AMC-K46 was determined as twice greater than that of the HeLa. The non-dividing density of both cell lines could be chosen from any density on the stable phase of the growth profile, starting from the confluent density (Figure 4.21). However, the spaces among the attached cells has been observed in the wells ranging from the confluent density of the 1.5×10^5 and 9×10^4 cells/well for the AMC-K46 and HeLa respectively (Figure 4.21). This was believed to be as the evidences of the "rippling effect" due to the pipetting and the moving of cultured plates after seeding. Therefore any densities on the stable phase without the rippling effect could be basically chosen as the optimum non-dividing density. Such the effect has never been found in the chosen densities; 2×10^5 and 10^5 cells/well for AMC-K46 and HeLa respectively. The effect has also never

been found on the higher densities than the chosen one for HeLa, but the lowest density was used due to the laboratory economic reason. The photographs of the optimum densities of both cell lines has been taken from the medium control group of the cells in a microtiter 96-wells plate and shown in Figure 4.22..

cells		AMC-K46	HeLa
Dividing density	cells / well	10^4	5×10^3
	cells / cm^2	2.6×10^4	1.3×10^4
Non-dividing density	cells / well	2×10^5	10^5
	cells / cm^2	5.2×10^5	2.6×10^5
Confluent (proliferated) density from the growth pattern (see 4.2)	cells / cm^2	1.13×10^5	1.86×10^5
Confluent (seeding) density from the OD_{MTT} (see 4.4.1 and Figure 4.18)	cells / well	9×10^4	7×10^4
	cells / cm^2	2.34×10^5	1.81×10^5

Table 4.2 The determined and calculated optimum densities of the two cell lines, AMC-K46 and HeLa. The calculation of the cell density from cells/well to cells/ cm^2 was based on the surface area of each well, 0.385 cm^2 (diameter = 0.7 cm).

To provide a clear figure about the cell densities of both cell lines, the comparison has been made and shown in Figure 4.22. The confluent density from the OD_{MTT} of AMC-K46 (2.34×10^5 cells/cm^2) was nearly twice to the confluent density from the growth pattern (1.13×10^5 cells/cm^2) (Table 4.2). The heterogeneous morphology of AMC-K46 among cell types with different growth rate should be an important reason. The confluent density from the OD_{MTT} of HeLa and the confluent density from the growth pattern were nearly equal (1.81×10^5 and 1.86×10^5 cells/cm^2, respectively). The homogeneous morphology of the HeLa with similar pattern of growth could be used to explain the nearly equal of the confluent density. However, the non-dividing density has been determined as twice greater than that of the dividing for both cell lines (see the cells/cm^2 for both in Table 4.2).

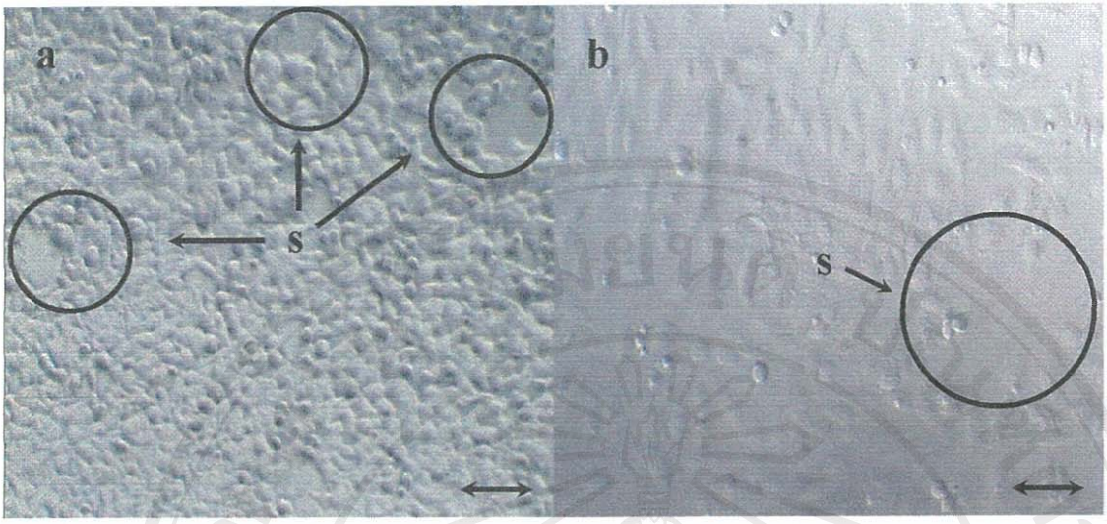

Figure 4.21 The rippling effects (seen as space (s)) has been observed among the attached cells in the confluent densities of both cell lines (a) AMC-K46 (9×10^4 cells/well) and (b) HeLa (7×10^4 cells/well) (scale bar = 50 μm).

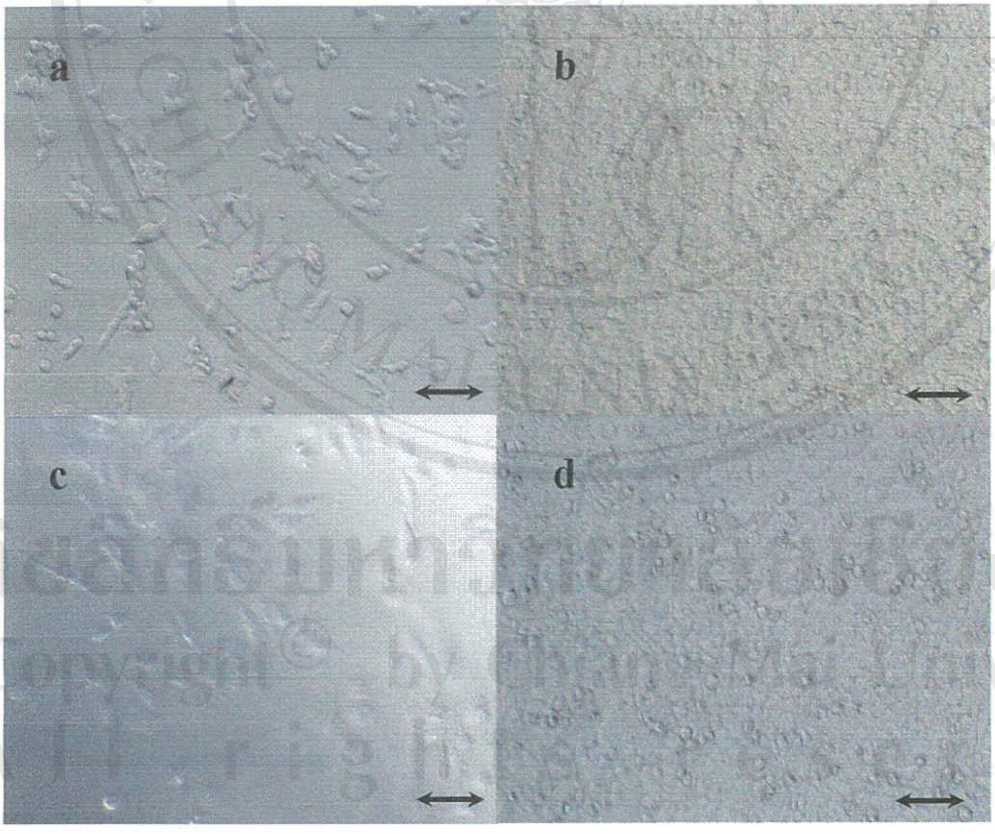

Figure 4.22 Photographs of the optimum cell densities of the two cell lines; (a) and (c) dividing cell densities, (b) and (d) non-dividing densities of AMC-K46 and HeLa, respectively. (scale bars = 100 μm)

4.4.2 The cytotoxicity assay of sodium dodecyl sulfate (SDS)

According to 3.3.2.3 (2), the ODs and the analysis by Priprobit 1.63 was shown in Appendix A. The MTT_{50} of the SDS to the two cell lines has been summarized in Table 4.3. The SDS contrarily effected to the two cell lines. The dividing AMC-K46 was effected at nearly two times (120.2 / 71.3 = 1.7 ~ 2) more than the non-dividing by SDS. The non-dividing HeLa seems to be effected by the SDS slightly higher than the dividing (127.8 / 104.4 = 1.2). However, these values of the SDS – MTT_{50} were used as the positive controls in the cytotoxicity assay for the plant crude extracts.

cell lines	SDS - MTT_{50} (μg/ml)	
	dividing density	non-dividing density
AMC-K46	71.3	120.2
HeLa	127.8	104.4

Table 4.3 The MTT_{50} of the sodium dodecyl sulfate (SDS) to the two cell lines.

4.5 The effect of the plant crude extracts to the two cell lines

4.5.1 Percent yield of the crude extracts

The percent yields were evaluated base on the 200 g of the dried powder of the plants as shown in Table 4.4. The crude extracts received by evaporation of the liquid extract at the temperature of 50 °C until the constant weight was obtained. The highest percent yield (16.18%) was belong to the leaves of *C. odorata* var. *fruticosa* and the least (6.89%) from the leaves of *A. reticulata.* The desired concentrations of crude-DMSO mixtures (CDM) and the preparation of crude-working solution (CWS) has shown in Table 4.5. These concentrations were used in accordance with those indicated in Figure 3.5.

Plant species	Weight of crude extracts (g)	Percent yield
A. reticulata (yf.)	22.55	11.28 %
A. reticulata (lv.)	13.75	6.89 %
A. reticulata (sb.)	22.47	11.24 %
A. squmosa (yf.)	16.96	8.48 %
A. squmosa (lv.)	22.14	11.07 %
C. odorata (lv.)	27.87	13.94 %
C. odorata var. *fruticosa* (lv.)	32.37	16.18 %
M. fruticosum (lv.)	31.42	15.71 %

Table 4.4 The percent yield of the dried ethanolic crude extract of the eight plants in family Annonaceae. (yf. =young fruit, lv. =leaves and sb. = stem bark)

Plant species	CDM (µg/ml)	CWS (µg/ml)						
		C1	C2	C3	C4	C5	C6	C7
A. reticulata (yf.)	50,000	500	400	300	200	100	60	20
A. reticulate (lv.)							nv	nv
A. reticulate (sb.)							nv	nv
A. squamosa (yf)							60	20
A. squamosa (lv.)							nv	nv
C. odorata (lv.)							nv	nv
C. odorata var. *fluticosa* (lv.)							nv	nv
M. fruticosum (lv.)							60	20

Table 4.5 The desired concentrations of the crude-DMSO mixtures (CDM) and the crude-working solution (CWS) of the plants. (yf. =young fruit, lv. =leaves, sb. = stem bark and nv = not available)

4.5.2 MTT assay of the plant crude extract

4.5.2.1 The activity assay and selective index evaluation

The MTT_{50} was determined and presented in Table 4.6 and 4.7 for AMC-K46 and HeLa respectively. The criteria of cytotoxicity activity for the crude extracts used in this study is as proposed by Tanamatayarat (2000). Three groups of the extracts has been classified; highly active, moderately active and no activity, with the value of MTT_{50}; ≤20, 21-100 and >100 μg/ml respectively.

To provide a more understanding of the activity of the extracts, the selectivity index has been evaluated and presented in Table 4.8. The criteria of the selectivity index has been proposed previously by Atindehou *et al.* (2004) and has been adapted in this research as the ratio of any two active or non-active MTT_{50} concentrations. In this research, the evaluation of the selectivity index is in three folds; highly selective, moderately selective and non-selective with the values ratio; ≤0.29, 0.3-0.79 and ≥0.8 respectively. This index provides a clear evaluation of any valuable lead compounds in the light of their ability to eliminate cancer cells but exert little damage to normal cells. The provisional good activity (or very highly selective) of the extracts is the <0.1 value of the ratio between dividing and non-dividing cells of the same cell line. The index has been calculated also between the two cell lines to estimate the activity of the lead compounds among the different targeted cells.

For AMC-K46 (Table 4.6), the most highly active extract was from the leaves of *M. fruticosum* with the MTT_{50} of 10.48 μg/ml to the dividings, but with $4.39x10^2$ μg/ml to the non-dividings. This means that the plant has a higher selective activity to kill the mitotic cells (dividing cells) than the resting cells (non-dividing cells) which indicated by the very low value of the selectivity index, 0.024 in Table 4.8. A moderated activity was detected from the young fruit of *A. squamosa* with almost similar MTT_{50}, 53.70 and 43.75μg/ml to the dividings and non-dividings respectively. Considering of this extract as a non selective activity between the dividings and non-dividings with the selectivity index >1 (53.70 / 43.75 = 1.23). The other extracts are all classified as no activity with the MTT_{50} >100 μg/ml and so have not been considered further in this research.

To the HeLa cells (Table 4.7), three extracts has shown the highly active effect to the dividings; *A. reticulata* (young fruits), *A. squamosa* (young fruits) and *M.*

fruticosum (leaves) with MTT_{50}; 0.86, 5.25 and 13.90 µg/ml respectively. The other three of the extracts expressed the moderately activity to the dividings; *A. reticulata* (leaves), *A. squamosa* (leaves) and *C. odorata var fruticosa* (leaves) with the MTT_{50}; 61.59, 82.30 and 74.90 µg/ml, respectively. For the non-dividing Hela, three extracts has been categorized as the moderately actives, *A. reticulata* (young fruits), *A. reticulata* (leaves) and *A. squamosa* (young fruits) with the MTT_{50}; 21.0, 96.3 and 59.24 µg/ml respectively. The Table 4.8 shows that; the *A. reticulata* (young fruit), *A. squamosa* (young fruit), *C. odorata var fruticosa* (leaves) and the *M. fruticosum* (leaves) expressed the highly selective to kill the dividings than the non-dividings with the selectivity index < 0.1. The other two extracts expressed moderately to less selectivity index to the dividings; *A. reticulata* (leaves) and *A. squamosa* (leaves) with the ratios, 0.640 and 0.814 respectively.

Plant species	MTT_{50} (µg/ml) on AMC-K46	
	Dividing cells	Non-dividing cells
A. reticulata (yf.)	$2.99x10^3$	$3.76x10^6$
A. reticulata (lv.)	$1.21x10^2$	$1.54x10^3$
A. reticulata (sb.)	$3.70x10^2$	$2.25x10^3$
A. squmosa (yf.)	53.70	43.75
A. squmosa (lv.)	$1.22x10^2$	$2.06x10^4$
C. odorata (lv.)	$1.06x10^4$	$3.55x10^5$
C. odorata var. *fruticosa* (lv.)	$3.64x10^2$	$1.21x10^3$
M. fruticosum (lv.)	10.48	$4.39x10^2$

Table 4.6 The MTT_{50} of the crude extracts on the AMC-K46. (yf. =young fruit, lv. =leaves and sb. = stem bark)

Plant species	MTT_{50} (μg/ml)on HeLa	
	Dividing cells	Non-dividing cells
A. reticulata (yf.)	0.86	21.0
A. reticulata (lv.)	61.59	96.3
A. reticulata (sb.)	$7.26x10^5$	$1.73x10^4$
A. squmosa (yf.)	5.25	59.24
A. squmosa (lv.)	82.30	$1.01x10^2$
C. odorata (lv.)	$1.01x10^4$	$1.15x10^7$
C. odorata var. *fruticosa* (lv.)	74.90	$2.86x10^3$
M. fruticosum (lv.)	13.90	$1.54x10^2$

Table 4.7 The MTT_{50} of the plants crude extracts on HeLa. (yf. =young fruit, lv. =leaves and sb. = stem bark)

Plant species	AMC-K46	HeLa	AMC-K46 vs HeLa	
			Dividing	Non-dividing
* *A. reticulata* (yf.)	NP	0.041	2.8×10^{-5}	5.5×10^{-6}
A. reticulate (lv.)	NP	0.640	0.51	0.063
* *A. squamosa* (yf)	NP	0.089	0.098	0.739
A. squamosa (lv.)	NP	0.814	0.675	NP
C. odorata var. *fluticosa* (lv.)	NP	0.028	0.206	NP
* *M. fruticosum* (lv.)	0.024	0.090	0.754	NP

Table 4.8 The selectivity index of the active extracts of the two cell lines calculated from the MTT_{50} presented in Table 4.3 and 4.4. The inactive extracts and the selective index values >1 are not presented in this table. (yf. = young fruit, lv. = leaves, NP = not presented (>1) and "*" = the chosen extracts to be used in genotoxic assay in 4.5.3)

Evaluating the selectivity index between the AMC-K46 and the HeLa cells (AMC-K46 vs HeLa), the dividings and non-dividings were separately considered (Table 4.8). The only one very highly selective extract between the two cell lines was from the young fruit of *A. reticulata* to both the dividings and non-dividings with the value of 2.8×10^{-4} and 5.5×10^{-6} respectively. However, the ratio was basically calculated from the MTT_{50} of no activity of the extract to the AMC-K46; 2.99×10^{3} and 3.76×10^{6} μg/ml for dividing and non-dividing respectively (see Table 4.6). This means that the lead compounds in the extract has a tendency to kill the HeLa cells in the culture much more effective than the AMC-K46. The other two very highly selective extracts with the ratio <0.1 were from the leaves of *A. reticulata* to non-dividings and the young fruit of *A. squamosa* to the dividings with the ratios of 0.063 and 0.098 respectively. The moderately selective extract was the leaves of *C. odorata var fruticosa* with 0.206 to the dividings. The other extracts apart from those indicated above expressed with a range of moderately selective (0.3-0.79) to non-selective (>0.8) between the two cell lines.

4.5.2.2 The chosen extracts from the MTT assay

In conclusion, the extracts with highly activity to kill AMC-K46 was from the leaves of *M. fruticosum* and with moderately active was the young fruit of *A. squamosa.* For the HeLa, the highly active extracts were from *A. reticulata* (young fruits), *A. squamosa* (young fruits) and *M. fruticosum* (leaves). Those with moderately active to HeLa were *A. reticulata* (leaves), *A. squamosa* (leaves) and *C. odorata var fruticosa* (leaves).The very highly more selective extracts to kill the HeLa than the AMC-K46 were *A. reticulata* (young fruit and leaves) and *A. squamosa* (young fruit). The only one moderated selective extract to both cell lines was *C. odorata var fruticosa* (leaves).

From the above cytotoxic assay and the selectivity index evaluation, the three extracts have been chosen to be used in the chromosome aberration assay (see 3.3.2.4 (2)) to the AMC-K46 cells (4.5.3); *A. reticulata* (young fruit), *A. squamosa* (young fruit) and *M. fruticosum* (leaves).

4.5.3 Effect of the chosen crude extracts to the AMC-K46 chromosome

According to the heterogeneity of the chromosome number of AMC-K46 (see 4.3), the study of chromosome aberration has been emphasized. The mitotic index and the chromosome aberration screening (type of aberration) had been studied.

4.5.3.1 The mitotic index

The average mitotic indexes (M.I.) of the crude extracts from the three plants, *A. reticulata* (young fruit), *A. squamosa* (young fruit) and *M. fruticosum* (leaves) are presented in Table 4.9. The M.I. of the cells treated with the extracts from *A reticulata* and *A. squamosa* exhibited (0.75 and 0.93 respectively) with non-significant difference from that of the Mitomycin C (MMC) treated cells (1.63). This explains that the two plant extracts inhibited the mitotic division of the cells. The extract from *M. fruticosum* exhibited (4.36) the same M.I. (with non-significant difference) to the DMSO treated cells (4.36) and the control cells (4.84). On considering the percentage of decreasing M.I. (P.D.M.I.), the cells treated with the extracts were 84.6, 80.9 and 10.2 for *A. reticulata*, *A. squamosa* and *M. fruticosum* respectively. The extracts from *A. reticulata* and *A. squamosa* expressed significantly higher anti-proliferative activity than the DMSO treated cells (P.D.M.I. =10.0). The extracts from the two plants also exhibited a non-significant difference of the P.D.M.I. to the MMC treated cells (P.D.M.I. = 66.3). The extract from *M. fruticosum* exhibited no effect to the cells with the P.D.M.I = 10.2 which is non-significant difference from the DMSO treated cells (P.D.M.I. =10.0).

4.5.3.2 The chromosome aberration

The chromosome aberration was screened from 232-345 metaphases and summarized in the Table 4.10. The percentage of the aberrant metaphase from the cells treated with *A. reticulata*, *A. squamosa* and *M. fruticosum* (0.82, 1.68 and 6.32, respectively) exhibited no significant difference to the DMSO and the medium control group (0.96 and 0.63 respectively). The numerical and structural mutation has been observed. The pattern of numerical changes in the cells after the exposure to the plant extracts shown in Figure 4.23-4.28. The total chromosome counting pattern of all treatment shown the 67 chromosomal cells still found in the highest frequency. The

68 chromosomal cells were decreased in the DMSO and the plant extract treatment groups.

There are 4 types of aberration observed in the cells treated with the crude extracts of the plants, the medium control and the solvent control (DMSO) groups; acentric fragment (ace) chromatid break (ctb), chromatid deletion (ctd) and chromatid gap (ctg) (Figure 4.29-4.33). All the 4 types of aberration were found in the cells treated with *A. reticulata*, while the ctb, and the ctb+ctd in *A. squamosa* and *M. fruticosum* treated cells respectively. The chromosome type of aberration in the crude extract treated cells was only found in one metaphase of the *M. fruticosum* group (Figure 4.33). In addition to the above four types of aberration, the chromosome break (acentric fragment or "ace") and the chromatid exchange (cte) were found in the MMC treated cells (with 59.29%). These aberrations are normally occurred in any animal cells treated with MMC (Klangsinsirikul, 2003) and in this study, AMC-K46.

	Control	DMSO	MMC	A. r.	A. s.	M. f.
M.I. (±S.D.)	4.84 (±2.27) [a]	4.36 (±0.27) [a]	1.63 (±0.08) [b]	0.75 (±0.25) [b]	0.93 (±0.26) [b]	4.35 (±0.68) [a]
D.M.I.	-	0.48 [c]	3.21 [d]	4.09 [d]	3.14 [d]	0.49 [c]
P-D.M.I.	-	10.0 [e]	66.3 [f]	84.6 [f]	80.9 [f]	10.2 [e]

Table 4.9 The effect of each crude extract to AMC-K46 proliferative activity (mitotic index):

M.I. = mitotic index

D.M.I. = decreasing of mitotic index of control group

S.D. = standard deviation of each group

P-D.M.I. = percentage of decreasing M.I. of AMC-K46 in each treatment

A. r. = *A. reticulata* (young fruit)

A. s. = *A. squmosa* (young fruit)

M. f. = *M. fruticosum*

MMC = mitomycin C

a, b, c, d, e and f = the different value with significant at level $p<0.05$

Treatment	Number of screened metaphase	Number of aberrant metaphases	percentage of aberration	Type of aberration
Control	322	2	0.63	ctb, ctd
DMSO	322	2	0.63	ctb, ctg
MMC	345	205	59.29	ctb, ctg, ctd, ace, cte
A. r.	232	5	0.82	ctb, ctg, ctd
A. s	243	2	1.68	ctb
M. f.	295	16	6.32	ctb, ctd, ace

Table 4.10 The effect of each crude extract to AMC-K46 chromosome.

A. r. = *A. reticulata* (young fruit)

A. s. = *A. squmosa* (young fruit)

M. f. = *M. fruticosum*

MMC = mitomycin C

ace = acentric fragment

ctb = chromatid break

ctd = chromatid deletion

cte = sister chromatid exchange (chromatid fusion)

ctg = chromatid gap

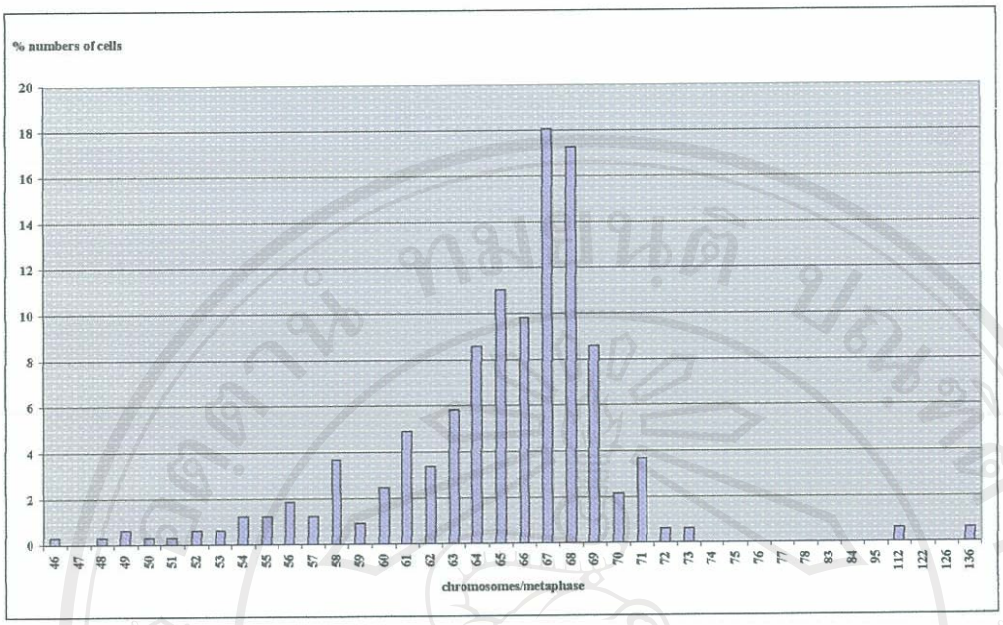

Figure 4.23 The total chromosome number pattern of AMC-K46, medium control group. The 67 chromosomes was the modal chromosome number.

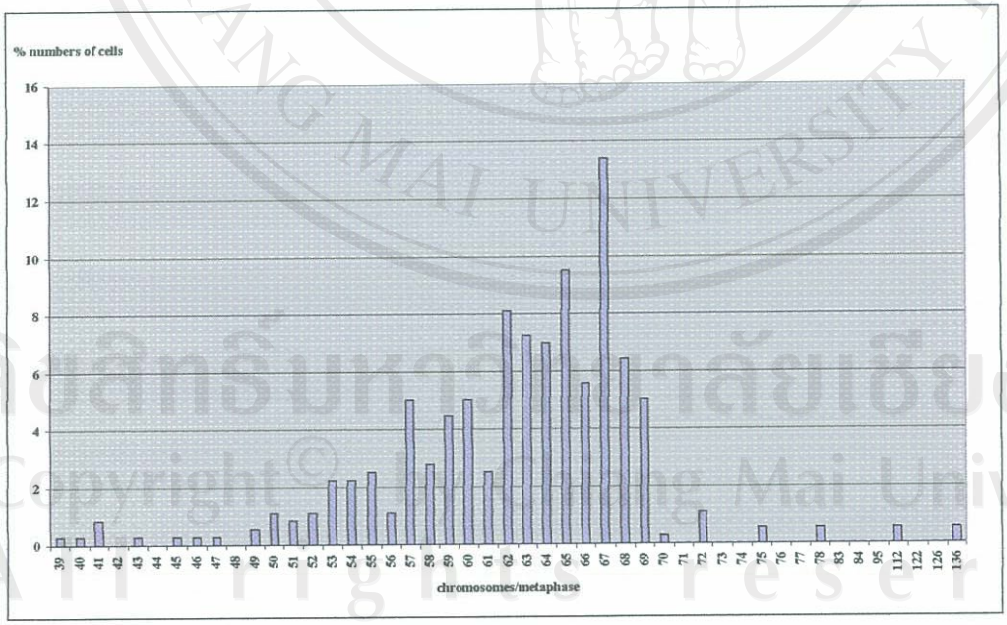

Figure 4.24 The total chromosome number pattern of AMC-K46, DMSO treated group. The 67 chromosomes was the modal chromosome number.

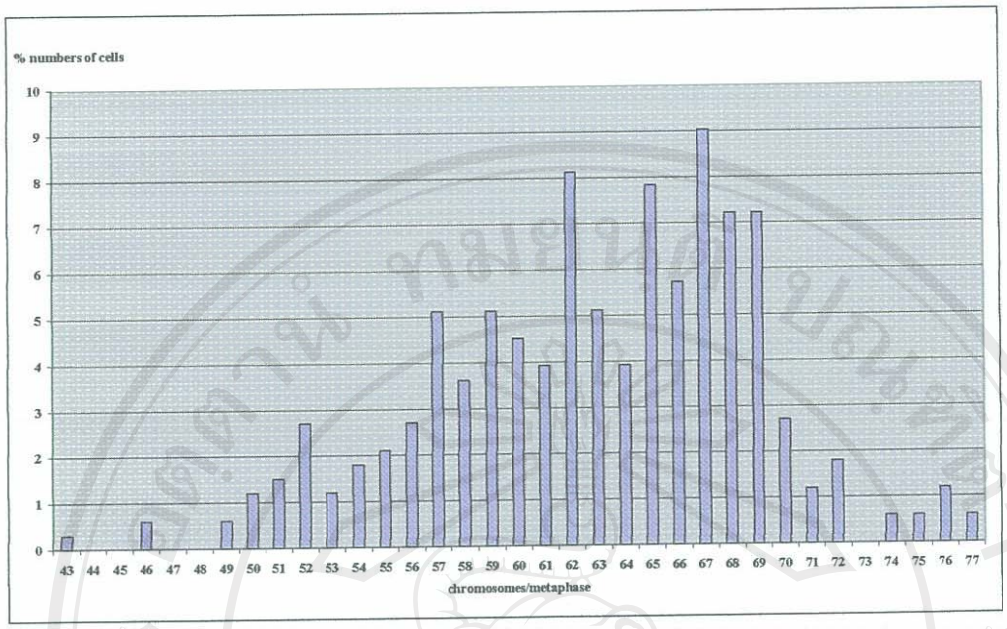

Figure 4.25 The total chromosome number pattern of AMC-K46, MMC treated group (positive control). The 67 chromosomes was the modal chromosome number.

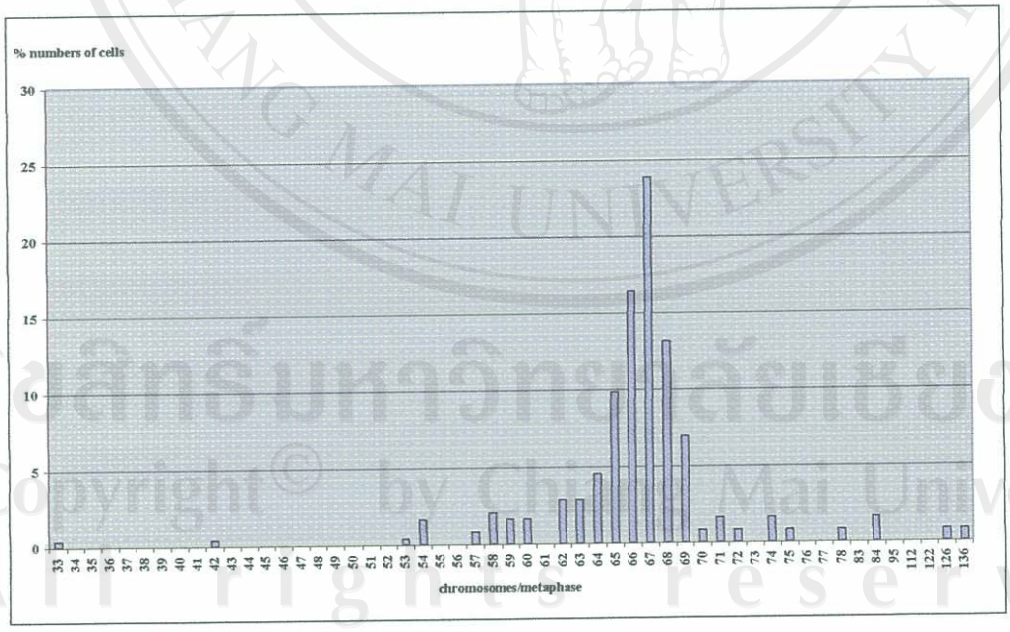

Figure 4.26 The total chromosome number pattern of AMC-K46, *A. reticulata* treated group. The 67 chromosomes was the modal chromosome number.

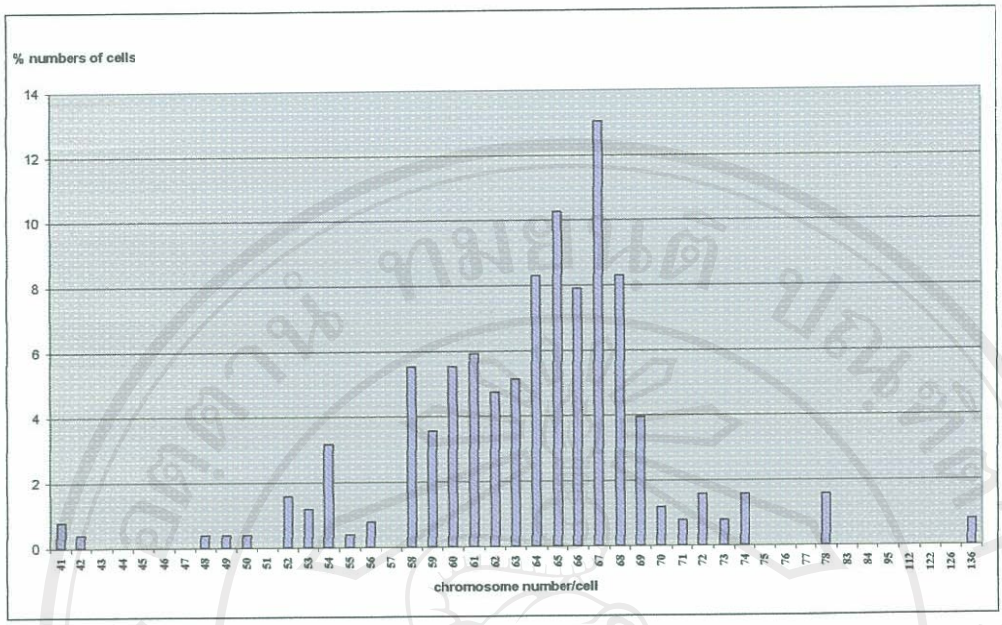

Figure 4.27 The total chromosome number pattern of AMC-K46, *A squamosa* treated group. The 67 chromosomes was the modal chromosome number.

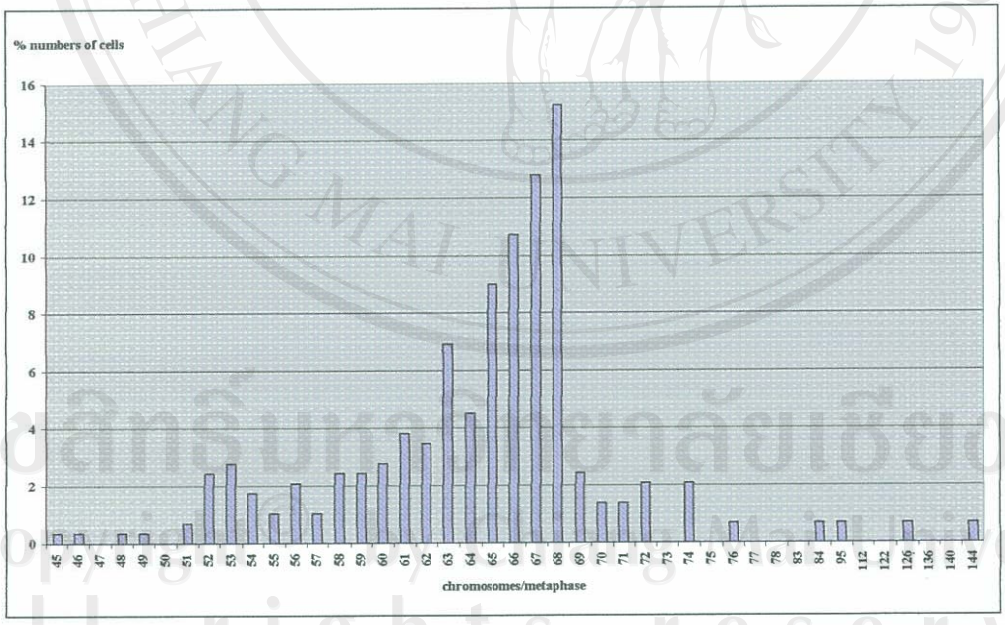

Figure 4.28 The total chromosome number pattern of AMC-K46, *M. fruticosum* treated group. The 67 chromosomes was the modal chromosome number.

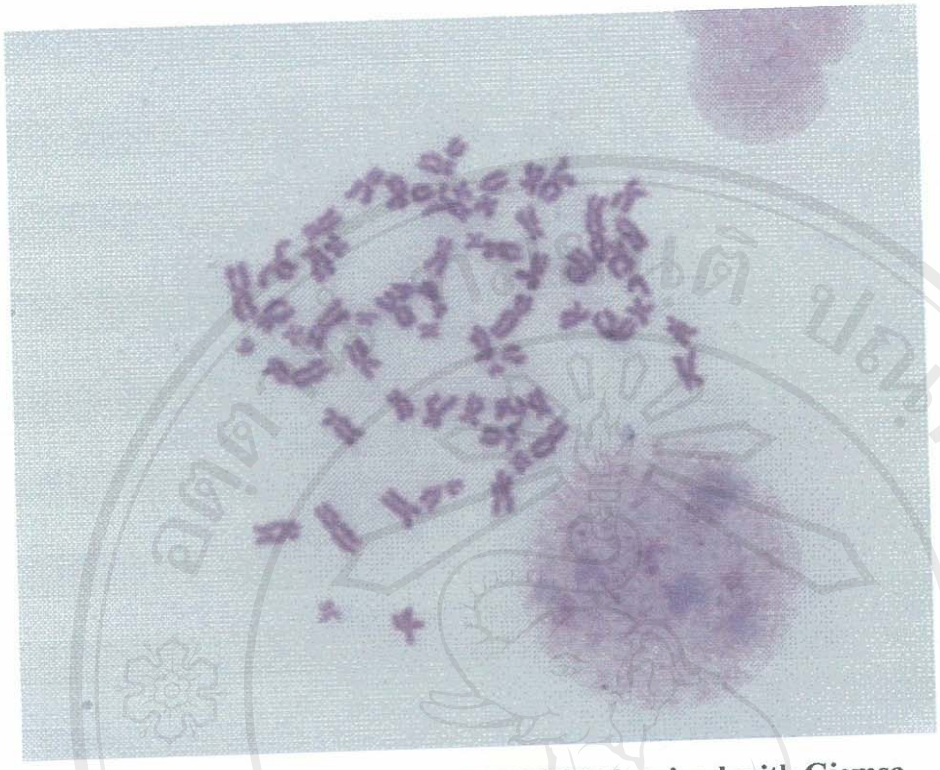

Figure 4.29 Metaphase chromosomes of AMC-K46 stained with Giemsa.

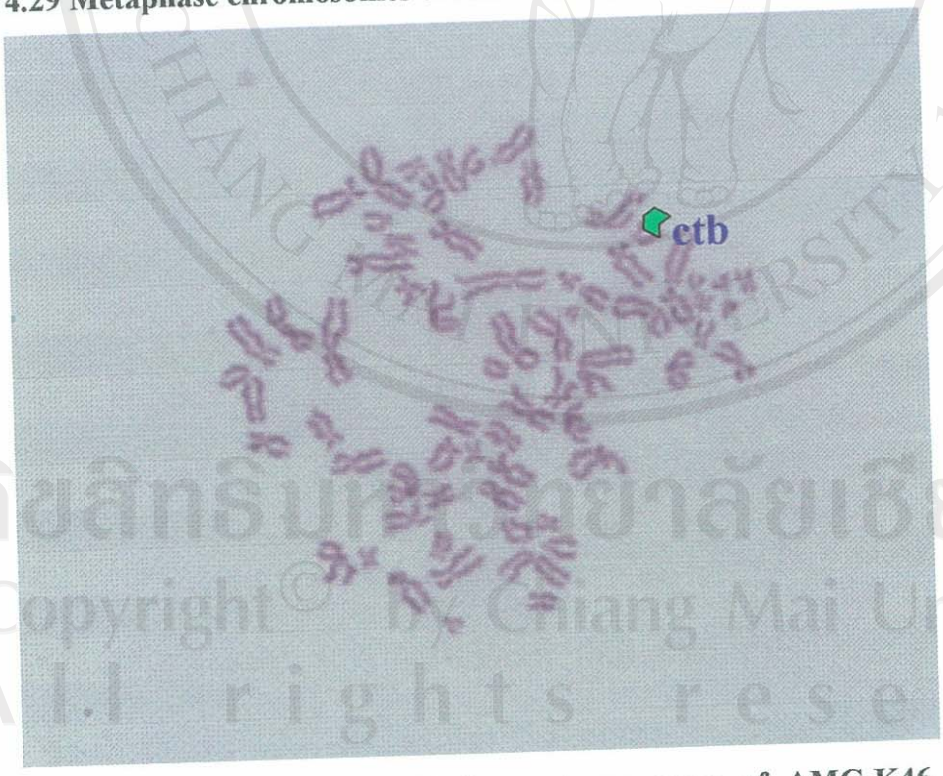

Figure 4.30 Chromatid break (ctb) in a chromosome of AMC-K46 in the negative control (DMSO).

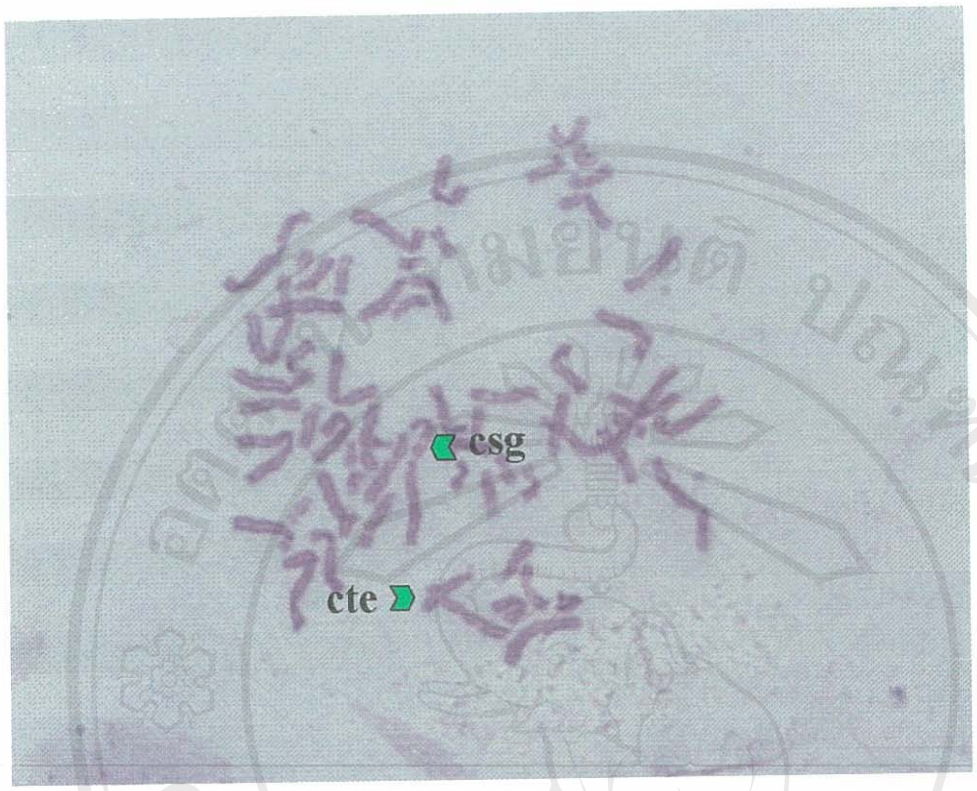

Figure 4.31 Chromosome aberration in MMC treatment group (64 chromosome) ; chromatid exchange (cte) and chromosome gap (csg).

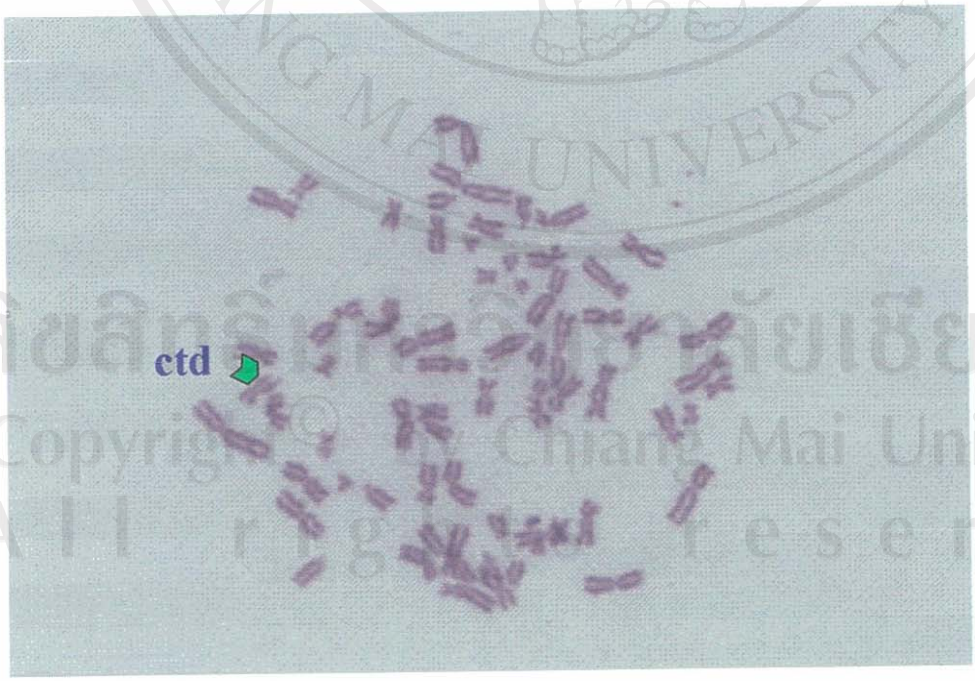

Figure 4.32 Chromosome aberration in the *A. reticulata* treatment group (68 chromosome); chromatid deletion (ctd).

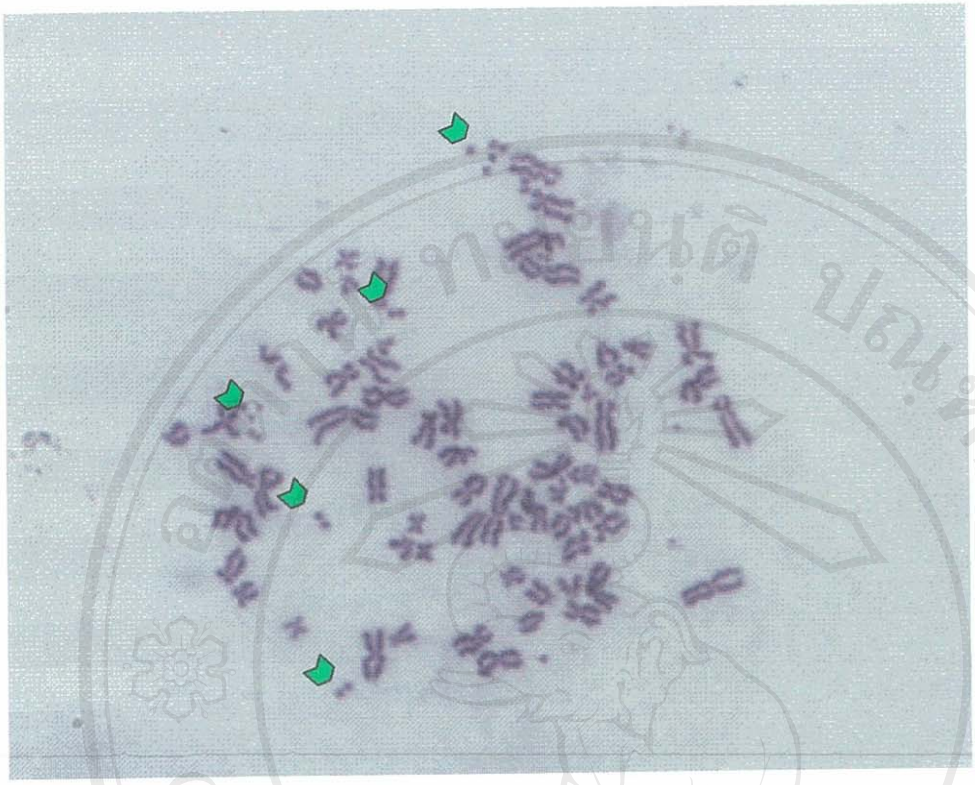

Figure 4.33 The chromosome aberration in crude extract of leaves of *M. fruticosum* treatment group: this metaphase found many acentric fragments.

4.5.4 The effect of crude extracts on the cell lines morphology

The two cell lines were treated with the active crude extracts of the plants (MTT_{50} ≤100 µg/ml). AMC-K46 was treated with the two extracts; *A. reticulata* (leaves) and *M. fluticosum* (leaves). HeLa was treated with the 6 active extracts; *A. reticulata* (leaves and young fruits), *A. squamosa* (leaves and young fruits), *C. odorata* var. *fruticosa* (leaves) and *M. fruticosum* (leaves). The cells were stained after the treatments and observed as previously describes in 3.3.2.4 (3).

Both cell lines responsed to all plant extracts in similar pattern.

Observation was made on the freshed cells of AMC-K46 (Figure 4.34). Rounding up of the cell shape was observed on the epitheloid cells exposed with the plant crude extracts. This rounding up phenomenon, somehow, could not indicate the shrinkage of the cells, although the cells seemed a bit smaller in size from the controled cells. Detachment of the cells from the cultured plates of more than half the number of attached cells in control groups has been estimated under the inverted

microscope. There was no different of cell morphology between the solvent control cells (DMSO treated) and the medium control cells. Similar morphological changes of the cells were also observed from the stained cells with Giemsa (Figure 4.35) to the freshed cells. Rounding up of nucleus was also observed in the extracts exposed cells with darker blue in colour than the control cells. The detachment of the cells was quite possible that the cells have loosen their ability to secrete the attached proteins.

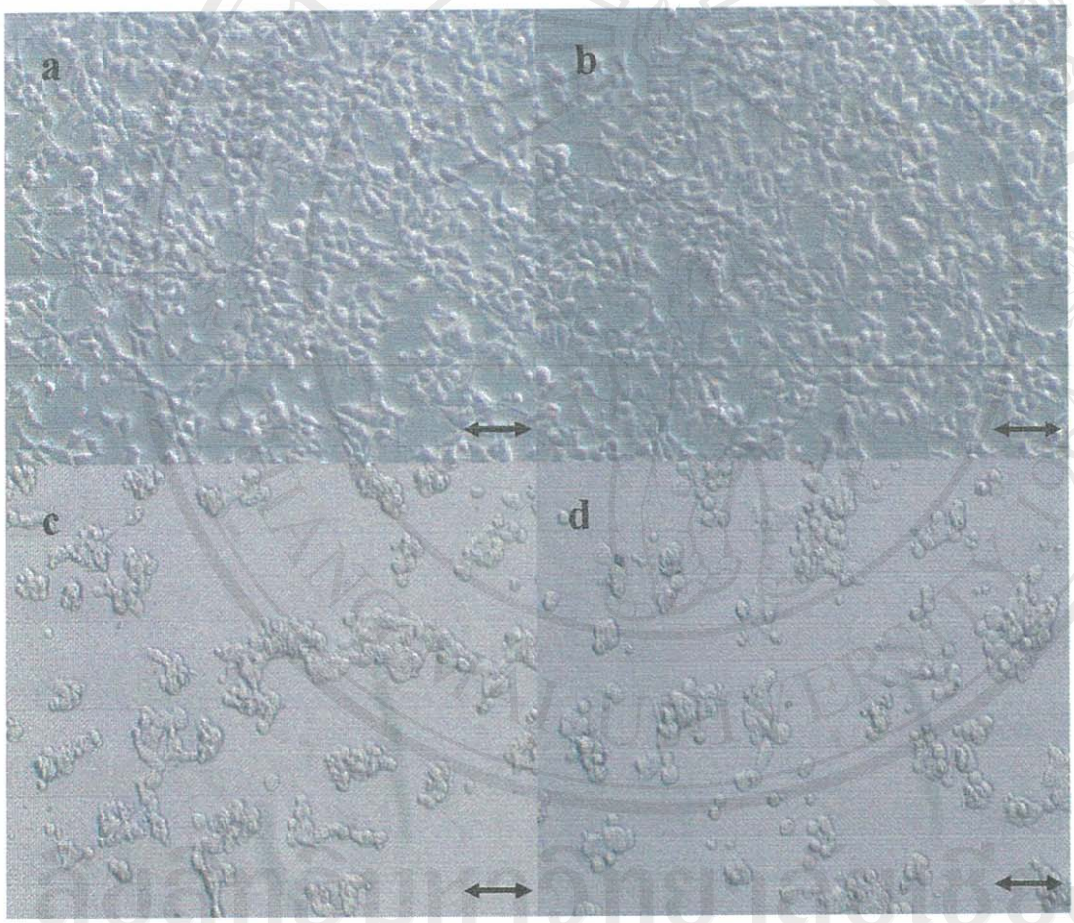

Figure 4.34 Morphological studied of AMC-K46 (a) control, (b) DMSO, (c) *A. squamosa* and (d) *M. fruticosum*. (scale bars = 100µm)

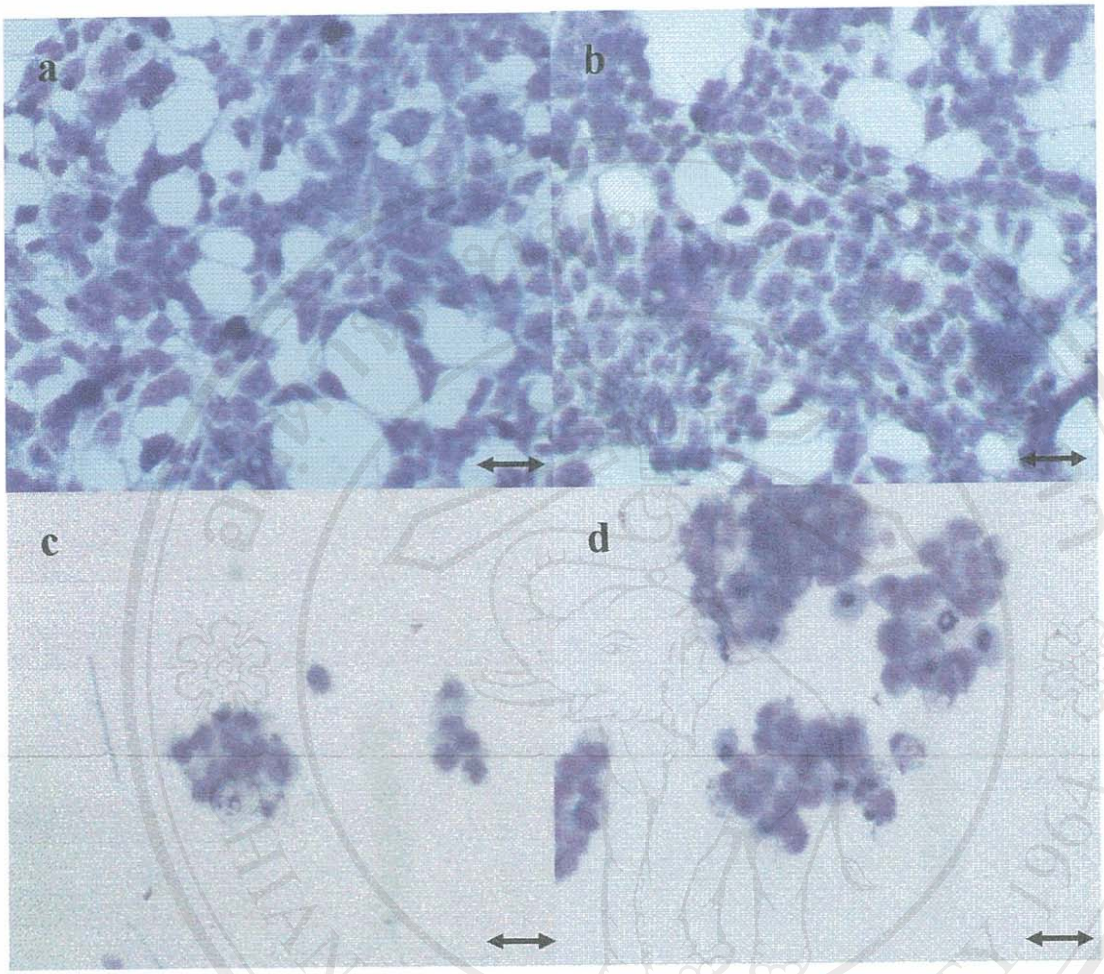

Figure 4.35 The morphological change in AMC-K46 stained with Giemsa (a) medium control, (b) DMSO, (c) *A. squamosa* and (d) *M. fruticosum.* (scale bars = 35 µm)

Normal shape of the HeLa cells has been observed from the solvent control and the medium control cells (Figure 4.36) with similar attached density. Both the freshed and stained survived cells from the extract treatment expressed similar phenomenon to the AMC-K46. The rounding up cells, the detachment of the cells from the cultured plates and the rounding up of nucleus with darker blue colour was occurred in the extracts treated groups (Figure 4.37). The more effected detachment of the cells in the cultures with *A. reticulata* (young fruits) has been observed than in the other extracts (Figure 4.36 (d) and 4.37 (d)).

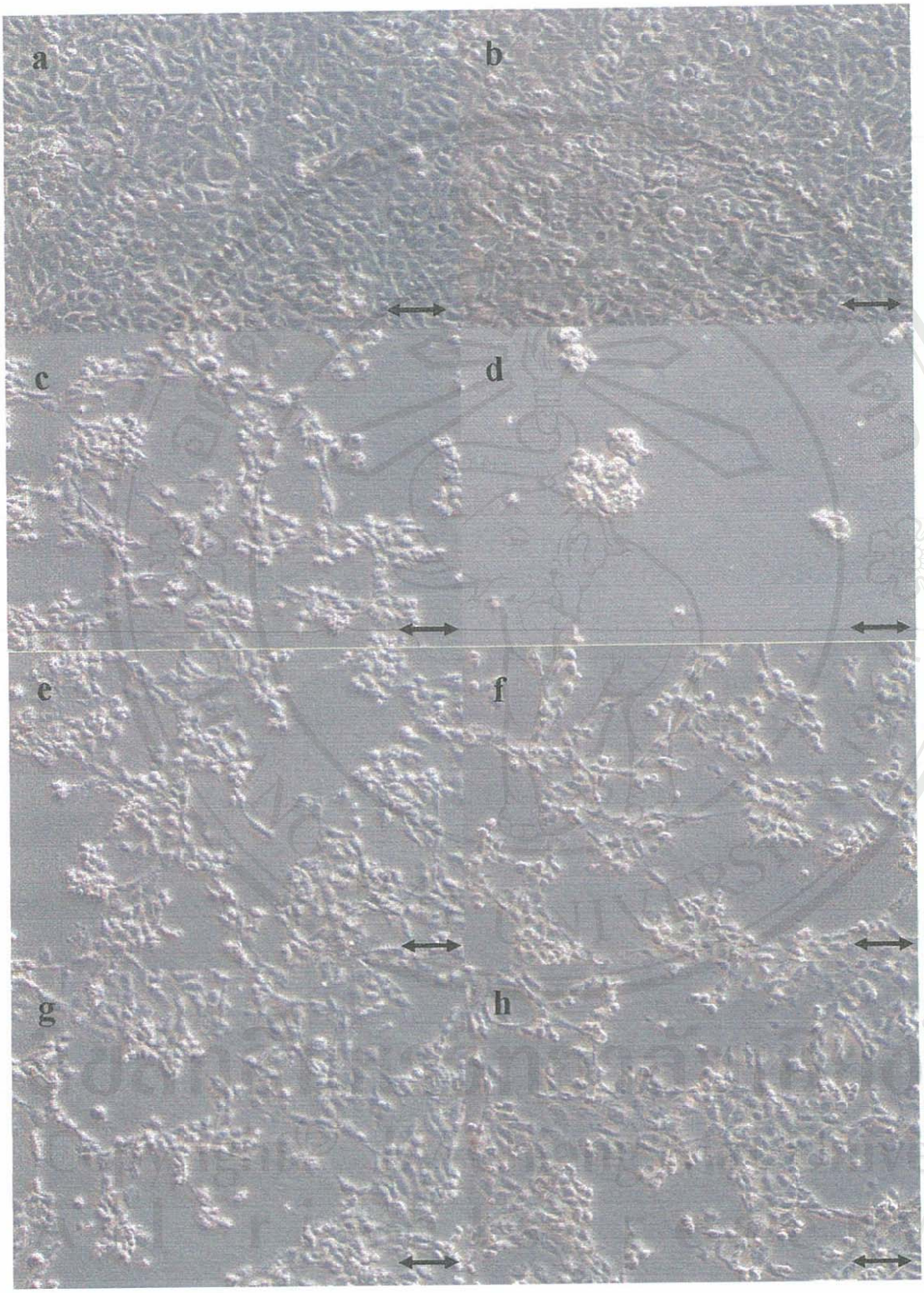

Figure 4.36 The morphological study of living HeLa; (a) medium control, (b) DMSO, (c) *A. reticulata* (leaves), (d) *A. reticulata* (young fruits), (e) *A squamosa* (leaves), (f) *A squamosa* (young fruits), (g) *C. odorata* var. *fruticosa* (leaves) and (h) *M. fruticosum* (leaves). (scale bars = 100μm)

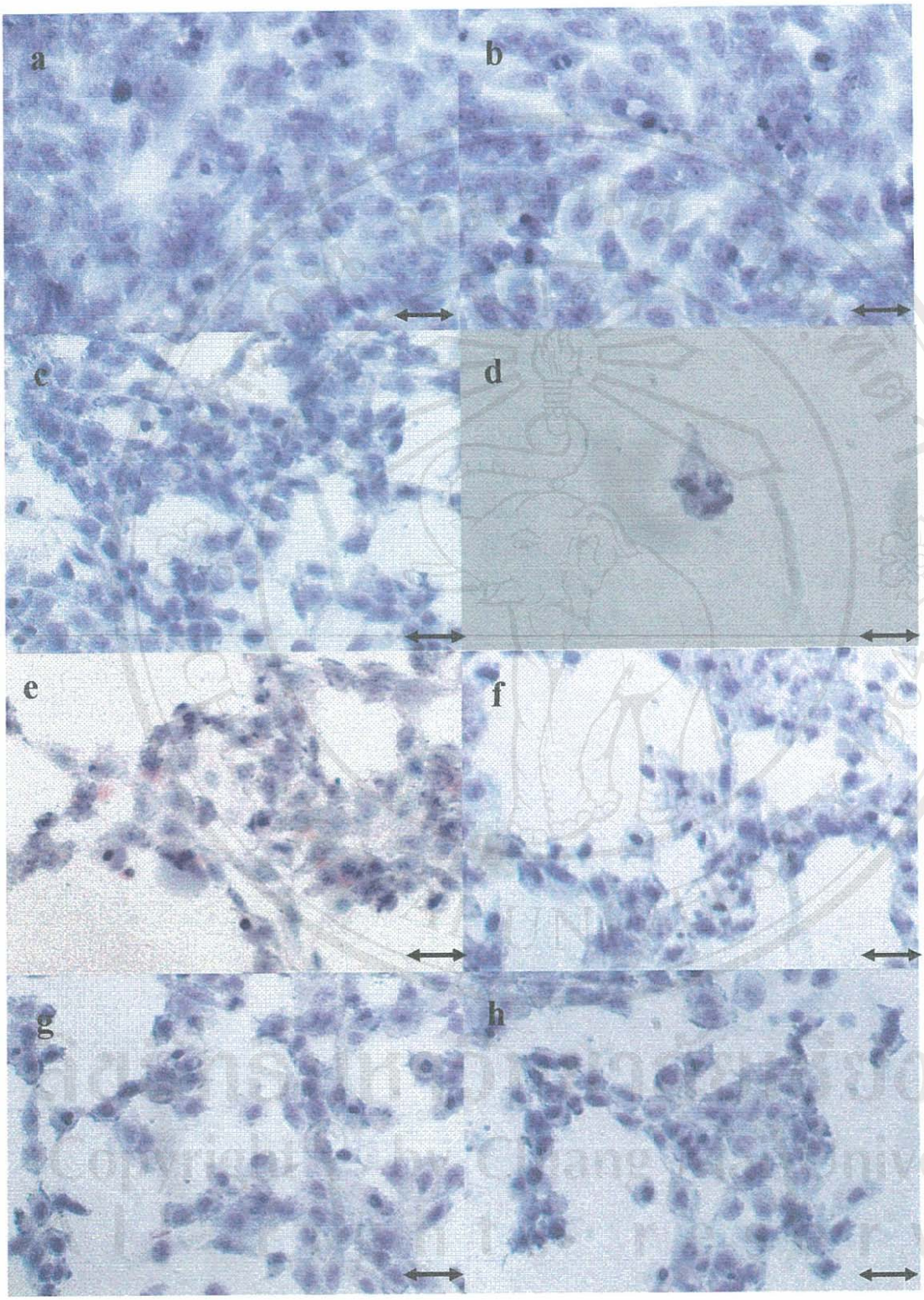

Figure 4.37 The morphological treatment of Giemsa stained HeLa; (a) medium control, (b) DMSO, (c) *A. reticulata* (leaves), (d) *A. reticulata* (young fruits), (e) *A squamosa* (leaves), (f) *A squamosa* (young fruits), (g) *C. odorata* var. *fruticosa* (leaves) and (h) *M. fruticosum* (leaves). (scale bars = 50μm)